

# 1 A study of $K^-d$ and $K^+d$ interactions via femtoscopy technique

2 W. RZESA <sup>(1)</sup>, ON BEHALF OF THE ALICE COLLABORATION

3 <sup>(1)</sup> *Warsaw University of Technology, Warsaw, Poland*

**Summary.** — Scattering cross section measurements have been used to study the strong interaction between charged kaons and (anti-)deuterons. However, these studies have not been successful in determining the scattering lengths of the strong interaction between  $K^+d$  and  $K^-d$ . Moreover, the currently available theoretical predictions for the  $K^-d$  scattering parameter are largely based on input from kaonic hydrogen measurements, while no theoretical predictions have yet been published for  $K^+d$ . In this work, the first measurements of the scattering lengths of  $K^+d$  and  $K^-d$  particle pairs are presented. The results were obtained using the femtoscopy technique which is very accurate for studying interactions between two particles with low relative momenta.

4

## 6 1. – Introduction

5

7 The femtoscopic study of particle correlations is a well-known method used to better  
 8 understand the interactions between the two particles under consideration, as well as to  
 9 study the characteristics of particle emitting sources. This paper focuses mainly on the  
 10 first of the two applications by studying the correlations of kaon–deuteron pairs. The  
 11 determination of the interaction parameters of the kaon–deuteron pairs can contribute to  
 12 the theoretical description of the strong interaction in low energy QCD as well as to the  
 13 obtaining of spin dependent scattering parameters in the strangeness sector. The scat-  
 14 tering parameters of the strong interaction could not be measured with other techniques  
 15 such as scattering or kaonic experiments. Moreover, from a theoretical point of view,  
 16 these parameters are either poorly known ( $K^-d$ ) or even unknown ( $K^+d$ ). Among many  
 17 systems already studied via the femtoscopy technique, the correlations with deuterons in  
 18 Pb-Pb collisions have never been experimentally checked. Kaon–deuteron studies were  
 19 recently done in pp collisions [1] but without measurements of scattering parameters.

## 20 2. – Femtoscopy and correlation functions

21 Femtoscopy of particle pairs studied via correlations as a function of their relative  
 22 momentum concerns particles in their final states [2]. The correlation function can be  
 23 defined by the Koonin-Pratt eq. (1):

$$(1) \quad C(\vec{k}^*) = \int S(\vec{r}^*) \left| \Psi(\vec{k}^*, \vec{r}^*) \right|^2 d^3r^*,$$

25 where  $\vec{k}^* = (\vec{p}_1 - \vec{p}_2)/2$  is a half of kaon–deuteron relative momentum in the pair rest  
 24

26 frame (PRF, the pair centre of mass is at rest,  $\vec{p}_1 = -\vec{p}_2$ ),  $\vec{r}^*$  is the relative separation  
 27 vector,  $S(\vec{r}^*)$  is two-particle emitting source function and  $\Psi(\vec{k}^*, \vec{r}^*)$  is the pair wave  
 28 function.

29 The source emission function describes the shape of the source and allows one to  
 30 estimate the size of the region of homogeneity that can be understood as an area from  
 31 which particles are emitted with similar velocities and directions. The usual approach in  
 32 such kind of analysis provides the standard description of experimental data by using the  
 33 Gaussian parametrization of the source. The source emission function can be described  
 34 according to:

$$(2) \quad S(\vec{r}^*) \sim \exp\left(-\frac{r^2}{2R_{Kd}^2}\right),$$

35 where  $R_{Kd}$  is a two-particle femtoscopic source size for non-identical particle pairs.

36 The wave function in the case of two particles has to take into account the quantum  
 37 statistics (if particles are identical) and final-state interactions - FSI (Coulomb interaction  
 38 in case the particles are charged, strong interaction in case the particles are hadrons). In  
 39 this analysis, the wave function are constructed from FSI without any quantum effects  
 40 as it concerns non-identical particles. The wave function for kaon–deuteron pairs can  
 41 be parametrized with the scattering length ( $f_0$ ) and the range of effective interaction  
 42 ( $d_0$ ) [3] in so called Lednický-Lyuboshitz model [4] expressed by the eq. (3):

$$(3) \quad |\psi(r^*, k^*)| = \sqrt{A_C(\eta)} [\exp(-ik^*r^*)F(-i\eta, 1, i\xi) + f_c(k^*)\frac{G}{r^*}],$$

43 where  $A_C$  is the Gamow factor expressed by  $\frac{2\pi}{k^*a_c} [\exp(\pm \frac{2\pi}{k^*a_c}) - 1]^{-1}$ ,  $F$  is the confluent  
 44 hypergeometric function,  $\eta = \frac{1}{k^*a_c}$ ,  $a_c$  is the pair Bohr radius,  $\xi = k^*r^* + \vec{k}^* \vec{r}^*$ ,  $G$  is a  
 45 combination of regular and singular s-wave Coulomb functions described in more detail  
 46 in [4] and  $f_c(k^*)$  is a scattering amplitude that can be expressed by the eq. (4),

$$(4) \quad f_C^{-1}(k^*) = \frac{1}{f_0} + \frac{1}{2}d_0k^{*2} - \frac{2}{a_C}h(k^*a_C) - ik^*a_C,$$

47 where  $h(x) = \frac{1}{x^2} \sum \frac{1}{n(n^2+x^2)} - C + \ln|x|$ .

48 In the experiment, the correlation function is calculated as the ratio of the distri-  
 49 butions of pairs of particles from the same collision and from two different collisions.  
 50 In the first case, the signal of the real correlation is naturally present, as the particles  
 51 have a chance to see each other. The second case is a reference distribution without any  
 52 correlation due to the interactions.

### 53 3. – Analysis detail

54 The results of kaon–deuteron femtoscopy study presented here are based on the anal-  
 55 ysis of data collected in 2018 during the Pb-Pb data-taking period at a center of mass  
 56 energy per nucleon pair  $\sqrt{s_{NN}} = 5.02$  TeV by the ALICE experiment [5, 6] working at  
 57 the LHC [7]. The study has been performed in three centrality intervals (0-10, 10-30,  
 58 30-50%) and two charge combination of pairs (pairs with antipairs were merged:  $K^+d$   
 59  $\oplus K^+\bar{d}$ ,  $K^-d \oplus K^-\bar{d}$ ). The main detectors used in the analysis are: Time Projection  
 60 Chamber (TPC [8]) and Time Of Flight detectors (TOF [9]) for identification of charged  
 61 particles, Inner Tracking System (ITS [10]) for better reconstruction of the primary ver-  
 62 tex and V0 detectors [11] for triggers (Minimum Bias, Central and Semicentral). For

63 this analysis, the primary vertex of the event had to be within 10 cm along the beam  
 64 direction from the centre of the ALICE detector. The transverse momentum ( $p_T$ ) range  
 65 of kaons in this analysis range for kaons taken to the analysis was 0.2 – 1.5 GeV/ $c$  and  
 66 for (anti-)deuterons was 0.8 – 2 GeV/ $c$ . The particles were also selected according to  
 67 their distance of closest approach (DCA) to the primary vertex and were accepted if  
 68 the DCA was smaller than  $\text{DCA}_{XY}(p_T) < 0.0105 + 0.0350/(p_T/(\text{GeV}/c)^{-1.1})$  cm. The  
 69 pseudo-rapidity ( $\eta$ ) for kaons and (anti-)deuterons was in the range  $|\eta| < 0.8$  <sup>(1)</sup>. All  
 70 track pairs, which share more than 5% of their total hits in the TPC, were excluded from  
 71 the analysis.

72 The correlation function of selected tracks is extracted after applying corrections for  
 73 non-femtoscopic background (i.e. collective motion of the system) and impurity effects  
 74 (quality of particle identification and fraction of primary particles). The non-femtoscopic  
 75 background was estimated by extrapolating the linear fit to the correlation function out-  
 76 side of the femtoscopic region. The corrections on imperfect particle identification and  
 77 not primary particles has been established based on both data-driven signal distribu-  
 78 tions and simulation studies. Two assumptions were made in the theoretical description.  
 79 First, the source is described by a Gaussian parametrization with a radius  $R$  shared be-  
 80 tween pairs of the same- and opposite-sign within each centrality interval. The effect of  
 81 possible non-Gaussianity has been taken into account following the procedure described  
 82 in [12] and simulation studies of LHYQUID [13] + THERMINATOR2 [14]. Second,  
 83 the zero-effective-range approximation ( $d_0=0$ ) is used. The imaginary and real parts of  
 84 the scattering length ( $f_0$ ) are the same for all centralities and are treated as free pa-  
 85 rameters (one scattering length value for same-signs and one for opposite-signs particle  
 86 pairs). Theoretical functions have been prepared following the Lednický & Lyuboshitz  
 87 model for different values of the radii and scattering parameters which creates a 3D (for  
 88 opposite-sign pairs) and 2D (for same-sign pair) grid with possible solutions. In order to  
 89 take into account the experimental momentum reconstruction, the theoretical functions  
 90 were smeared for the experimental momentum resolution. The fitting algorithm is based  
 91 on a minimum  $\chi^2$  of the data to model functions that is calculated simultaneously for  
 92 all centralities and charge combinations, as the parameters are shared between functions  
 93 (see similar study [15]). The final result of the analysis is composed of three different  
 94 values of the femtoscopic radius at each centrality interval and two scattering lengths ( $\Re$   
 95 and  $\Im f_0$  for opposite-sign pairs,  $\Re f_0$  for same-sign pairs).

#### 96 4. – Results

97 The correlation functions together with the fit in three centrality classes of  $K^-d \oplus K^+\bar{d}$   
 98 and  $K^+d \oplus K^-\bar{d}$  pairs are shown in Fig. 1. It is clear that we can reproduce the data  
 99 using the Lednický-Lyuboshitz model. The parameters derived in presented fit are the  
 100 first experimental measurements of kaon–deuteron scattering lengths:

$$101 \begin{aligned} K^-d: \Re f_0 &= -1.52 \pm 0.16(\text{stat})_{-0.08}^{+0.04}(\text{syst}), \\ &\Im f_0 = 1.01 \pm 0.23(\text{stat})_{-0.15}^{+0.07}(\text{syst}), \\ 103 K^+d: \Re f_0 &= -0.58 \pm 0.12(\text{stat})_{-0.12}^{+0.14}(\text{syst}). \end{aligned}$$

104 The values of measured scattering parameters were compared in Fig. 2 to available the-  
 105 oretical predictions. The predictions for  $K^-d$  pairs come mainly from calculations that  
 106 used inputs of kaonic hydrogen scattering parameters [16, 17, 18, 19, 20, 21]. The  $K^+d$

---

<sup>(1)</sup> $\eta = -\ln\left(\text{tg}\left(\frac{\theta}{2}\right)\right)$ , where  $\theta$  is the angle between the particle momentum and the beam axis.

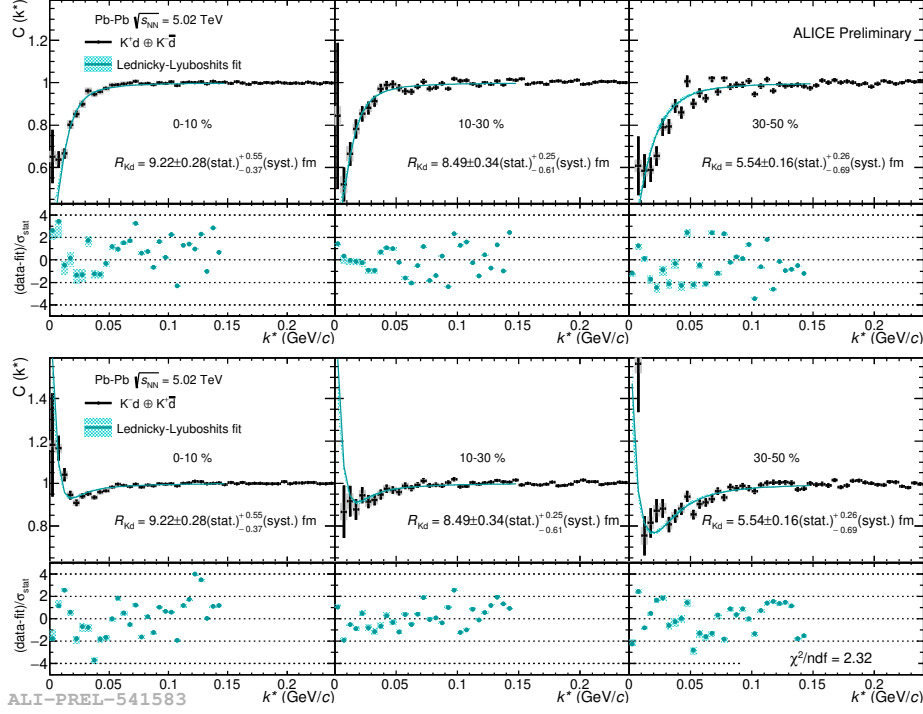


Fig. 1. – Points represents correlation functions for  $K^+d \oplus K^-\bar{d}$  (upper row) and  $K^-d \oplus K^+\bar{d}$  (bottom row) pairs in Pb–Pb collisions at  $\sqrt{s_{NN}} = 5.02$  TeV for three centrality classes, from left to right: 0–10%, 10–30%, 30–50%. Lines show the fit functions of Lednický–Lyuboshitz model. Lower panels present the difference between the data and model functions divided by the statistical uncertainties of data points.

107 scattering values derived in this work are compared to theoretical calculations provided  
 108 within private communication with prof. Tetsuo Hyodo and prof. Johann Haidenbauer  
 109 as currently there is no published theoretical prediction for this pair combination.

110 The source radii obtained within simultaneous fit are presented in Fig. 3 as a func-  
 111 tion of the cube root of charged-particle multiplicity density. The radii for kaon–deuteron  
 112 pairs from Pb–Pb collisions are between 5 and 10 fm. A clear growing trend can be ob-  
 113 served, with the size of homogeneity rising with more central collisions.

## 114 5. – Summary

115 The femtосcopy analysis of pairs of charged kaons and (anti-)deuterons on data from  
 116 Pb–Pb collisions with ALICE at the LHC allowed for first measurements of the unknown  
 117 scattering parameters of the strong interaction between  $K^+ \bar{d}$  and  $K^- d$  pairs in a unique  
 118 way. The obtained parameters are in agreement with most of theoretical calculations.  
 119 The study provides also estimation of the radii of the particles emitting source of kaon–  
 120 deuteron pairs in Pb–Pb collisions.

121

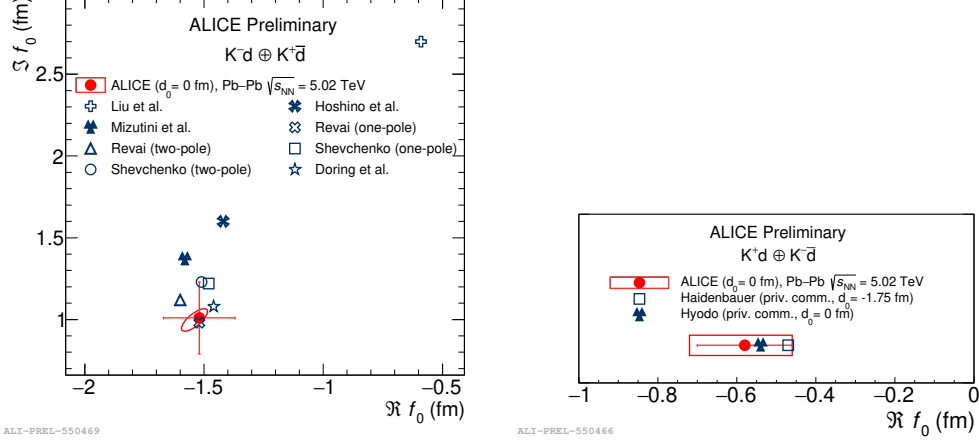


Fig. 2. – Left: comparison of the  $K^-d \oplus K^+\bar{d}$  scattering length values measured in Pb–Pb collisions at  $\sqrt{s_{NN}} = 5.02$  TeV shown with red circles together with the theoretical predictions derived by [16, 17, 18, 19, 20, 21] shown with blue markers. Right: comparison of the  $K^+d \oplus K^-\bar{d}$  scattering length values measured in Pb–Pb collisions with red circles together with the theoretical predictions derived by prof. T. Hyodo and J. Haidenbauer within private communication.

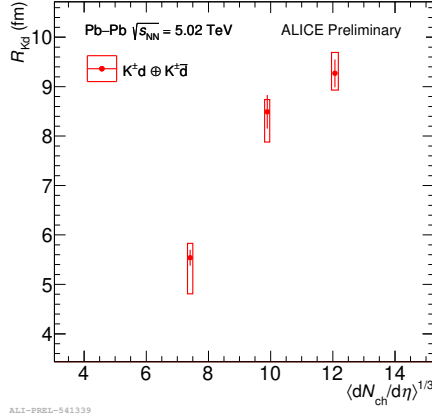


Fig. 3. – Radii as a function of  $\langle dN_{ch}/d\eta \rangle^{1/3}$  measured in Pb–Pb collisions at  $\sqrt{s_{NN}} = 5.02$  TeV in a simultaneous fit to all kaon–deuteron pair combinations.

122

\* \* \*

123 Many thanks to prof. Tetsuo Hyodo and prof. Johann Haidenbauer for consent to  
 124 use their theoretical predictions of  $K^+d$  scattering lengths for comparison with value  
 125 obtained within this study.

126 This work is funded by the IDUB YOUNG-PW programme at Warsaw Univer-  
 127 sity of Technology and by the Polish National Science Centre under agreements no.  
 128 2022/45/B/ST2/02029, and no. 2023/49/N/ST2/03525

## 129 REFERENCES

- 130 [1] A. Collaboration *arxiv nucl-ex 2308.16120*.  
131 [2] M. Lisa *et al. Annual Review of Nuclear and Particle Science*, vol. 55, no. 1, 2005.  
132 [3] A. Kisiel *Braz.J.Phys.*, vol. 37, pp. 917–924, 2006.  
133 [4] R. Lednicky *et al. Sov. J. Nucl. Phys.*, vol. 35, p. 770, 1982.  
134 [5] K. Aamodt *et al. JINST*, vol. 3, p. S08002, 2008.  
135 [6] B. B. Abelev *et al. Int. J. Mod. Phys. A*, vol. 29, p. 1430044, 2014.  
136 [7] L. Evans and P. Bryant, “LHC Machine,” *JINST*, vol. 3, p. S08001, 2008.  
137 [8] P. Gasik *Nucl. Phys. A*, vol. 982, pp. 943–946, 2019.  
138 [9] A. Akindinov *et al. Eur. Phys. J. Plus*, vol. 128, p. 44, 2013.  
139 [10] K. Aamodt *et al. JINST*, vol. 5, p. P03003, 2010.  
140 [11] E. Abbas *et al. JINST*, vol. 8, p. P10016, 2013.  
141 [12] A. Kisiel. PhD thesis, Warsaw U. of Tech., 2004.  
142 [13] B. žek *et al. Phys. Rev. C*, vol. 85, p. 064915, Jun 2012.  
143 [14] M. Chojnacki *et al. Computer Physics Communications*, vol. 183, no. 3, pp. 746–773, 2012.  
144 [15] S. Acharya, D. Adamová, A. Adler, J. Adolfsson, and G. A. A. COLLAB *Physics Letters B*, vol. 822, p. 136708, 2021.  
145 [16] Z.-W. Liu *et al. Physics Letters B*, vol. 808, p. 135652, 2020.  
146 [17] T. Hoshino *et al. Phys. Rev. C*, vol. 96, p. 045204, Oct 2017.  
147 [18] T. Mizutani *et al. Phys. Rev. C*, vol. 87, p. 035201, Mar 2013.  
148 [19] J. Révai *Few-Body Systems*, vol. 54, p. 135652, 2013.  
149 [20] N. V. Shevchenko *Few-Body Systems*, vol. 54, pp. 1187–1189, 2013.  
150 [21] M. Döring *et al. Physics Letters B*, vol. 704, no. 5, pp. 663–666, 2011.